Impact of Depth-Wise Inhomogeneous Iron Distributions on the Accuracy of Lifetime-Based Interstitial Iron Measurements on Silicon Wafers

Tien T. Le [ID], Sieu Pheng Phang, Zhongshu Yang [ID], Daniel Macdonald [ID], *Senior Member, IEEE*, and AnYao Liu [ID]

Abstract—This article studies the impact of depth-wise inhomogeneous iron distributions in silicon wafers, and the magnitude of the average iron concentrations, on the accuracy of interstitial iron concentrations extracted from effective lifetime measurements on crystalline silicon wafers. The depth-wise inhomogeneous interstitial iron profiles are generated from simulations of gettering of iron to the wafer surfaces, and are therefore practically relevant for silicon solar cells. Our analysis shows that a considerable amount of error can be introduced into the interstitial iron concentration measurement if the iron profiles are highly inhomogeneous, such as in the early stages of gettering. The absolute interstitial iron concentration also has a determinant role on the magnitude of the error. A "threshold" interstitial iron concentration of 10^{13} cm^{-3} or below ($<10^{13}$ cm^{-3}) is recommended for defect studies to avoid significant measurement errors. Other effects such as surface passivation, light source spectrum and wafer thickness are found to also affect the accuracy of the interstitial iron concentration measurement by affecting the uniformity of the carrier profiles.

Index Terms—Carrier lifetime, gettering, iron, QsCell, quasi-steady state photoconductance (QSSPC), silicon, simulations.

I. INTRODUCTION

IRON (Fe) is one of the most common and important impurities in silicon (Si) based devices, such as silicon solar cells. The presence of Fe can be very detrimental to the function of Si solar cells due to its high recombination activity. Iron has a moderately fast diffusivity in Si, making solar cells susceptible to iron contamination during processing [1]. Therefore, it is important to be able to accurately detect and measure Fe in Si wafers.

A wide range of techniques have been demonstrated to measure Fe in Si, as summarized in [1] and [2], including minority carrier lifetime-based techniques [3], [4], deep level transient spectroscopy [5], total reflection X-ray fluorescence [6], and atomic absorption spectroscopy or mass spectrometry [7], [8]. However, for a fast and non-destructive measurement of the dissolved interstitial Fe in Si, which in most cases is the most harmful form of Fe, interstitial Fe in Si is commonly measured by using the technique of carrier lifetimes, or diffusion lengths, based on the lifetimes measured before and after the dissociation of FeB pairs [3], [4], [9]. This widely used technique is made possible due to the reversible pairing/un-pairing reaction between interstitial Fe (Fe_i) and substitutional boron (B_s) in p-type Si. The dissociation of FeB can be easily facilitated either by thermal annealing or optical activation (via strong illumination) [3], [4]. This lifetime-based technique allows a sensitive measurement of the interstitial Fe concentration in Si (simply referred to as Fe concentration or [Fe] in the rest of this article).

One important assumption of the lifetime-based techniques is that the depth-wise carrier profiles in silicon wafers are assumed homogeneous, as the effective lifetimes before and after FeB dissociation are used to estimate the Fe concentration in Si. However, for a low lifetime sample, the carrier diffusion length may be comparable to or even smaller than the wafer thickness, and the resulting depth-wise carrier profile is inherently non-uniform. This non-uniformity can also result from different excitation wavelengths or spectra of the illumination sources, different surface passivation quality, or the effect of other impurities and crystal defects as illustrated in Schubert et al. [10]. As reported by Schubert et al. [10], such non-idealities can lead to extremely non-uniform carrier profiles, and consequently introduce a significant error into the Fe measurement using lifetime-based techniques, with possible errors up to a factor of 2 (∼100% error).

Though Schubert et al. [10] studied a range of possible scenarios that can affect the depth-wise uniformity of the carrier profiles and simulated the subsequent impact on the lifetime-based [Fe] measurement, their work only considered the case of a homogenous Fe distribution in the Si wafer bulk. However, as most solar cells incorporate some level of gettering to the wafer surface region during processing, e.g., from phosphorus diffusion, polysilicon/oxide activation, dielectric film deposition and activation, or aluminium alloying [11], the resulting depth-wise distribution of Fe in Si wafers can be largely inhomogeneous. In addition, due to its ease of detection, Fe is commonly used as a tracer impurity in silicon to study the effects of various gettering sinks. Therefore, the impact of a non-uniform Fe profile on

the accuracy of the Fe measurement should be assessed. The work by McLean et al. considered this effect, but simplified the simulations by assuming a very simple three-step Fe profile using PC1D [12]. In addition, McLean et al. [12] only examined an average Fe concentration of 10^{12} cm^{-3}. As shown by Schubert et al. [10], the Fe concentration ([Fe]) itself also significantly affects the uniformity of the carrier profiles.

In this article, we carry out simulations to examine the impact of a depth-wise nonuniform Fe distribution on the accuracy of the Fe estimation from effective lifetime measurements. The nonuniform Fe profiles are derived from simulations of a surface gettering process [13], and therefore the profiles are practically relevant and representative of real solar cell fabrication. A range of Fe concentrations are examined to identify the "threshold" concentration below which errors are acceptable, especially for gettering studies. The carrier density profiles were simulated using QsCell [14], [15], [16], [17]. The effect of other factors such as surface recombination, optical generation profile, and wafer thickness variation are also simulated and discussed.

II. SIMULATION DETAILS

A. Simulation Procedure and Input Parameters

This article used the previously reported QsCell approach [14], [15], [16], [17] with the introduction of a depth-wise inhomogeneous distribution of Fe [Fe(x)] in the Si wafer. Consequently, instead of homogeneous Shockley–Read–Hall (SRH) electron and hole minority carrier lifetimes (homogeneous τ_{n_0} and τ_{p_0} throughout the wafer thickness), both τ_{n_0} and τ_{p_0} become depth-dependent functions of Fe(x). The following SRH parameters were used to estimate τ_{n_0} and τ_{p_0} from the input Fe$_i$ and FeB concentrations: $\sigma_{n,Fe_i} = 1.3 \times 10^{-14}$ cm^{-2}, $\sigma_{p,Fe_i} = 7 \times 10^{-17}$ cm^{-2}, $E_{t,Fe_i} - E_V = 0.380\,eV$ for interstitial Fe$_i$ [18], [19], and $\sigma_{n,FeB} = 5.0 \times 10^{-15}$ cm^{-2}, $\sigma_{p,FeB} = 3.0 \times 10^{-15}$ cm^{-2} and $E_C - E_{t,FeB} = 0.260\,eV$ for FeB [20]. The input Fe(x) distribution profiles are discussed in the next section (see Section II-B).

By solving the continuity equation with the open-circuit constraint such that the total current $J = 0$, the carrier depth profile $\Delta n(x)$ can be obtained [14], [15]. $\Delta n(x)$ was obtained by varying the generation rate until an average carrier concentration of $\Delta n = \frac{\int_0^W \Delta n(x)dx}{W} = 1 \times 10^{15}$ cm^{-3} was satisfied, where W is the wafer thickness. An average $\Delta n = 1 \times 10^{15}$ cm^{-3} was chosen because this is a commonly used injection level to measure the effective lifetimes used to estimate the Fe concentrations. The effective lifetime ($\tau_{\rm eff}$) at the average injection level (Δn) under quasi-steady-state conditions, which is the mode generally used to measure the low-lifetime samples containing Fe, is calculated by [14], [15], [16], [17]

$$\tau_{\rm eff}\,(\Delta n) = \frac{\Delta n}{G_L} \qquad (1)$$

where $G_L = \frac{\int_0^W {\rm G}(x)dx}{W}$ (cm^{-3}) is the average generation rate and G(x) (cm^{-3}) is the generation profile in the Si wafer bulk.

For the comparison among PC1D [12], modified QsCell simulation and the results of Schubert et al. [10], a monochromatic

illumination source of 790 nm was assumed (see Section III-B). For the Fe concentration error analyses, the standard Xenon flash spectrum [21] in the commonly used QSS photoconductance lifetime tester from Sinton Instruments was used [17], [22]. Only the magnitude of $G(x)$ was varied, not its depth profile.

In the error analyses, we assumed a p-type wafer with a boron doping concentration of $N_A = 1 \times 10^{16}$ cm^{-3} and a wafer thickness of 300 μm (unless otherwise specified), which is the condition commonly used in our gettering studies. We assumed two different surface passivation conditions: "well passivated samples" in this article refer to the case of a very small surface saturation current density (J_0) of $J_{0f} = J_{0b} = 10^{-15}\,A{\rm cm}^{-2}$, where J_{0f} and J_{0b} refer to the front and back side J_0, respectively; and "poorly passivated samples" refer to the case of a high $J_{0f} = J_{0b} = 10^{-13}\,A{\rm cm}^{-2}$. All of the effective lifetimes were calculated at an average injection level of $\Delta n = 1 \times 10^{15}$ cm^{-3}.

For each input Fe(x) profile, the average effective lifetimes [from (1)] in the fully dissociated Fe$_i$ and fully associated FeB states, $\tau_{\rm eff,\,Fe_i}$ and $\tau_{\rm eff,\,FeB}$ respectively, were then used to calculate the average Fe concentration [3], [4]

$$[{\rm Fe}]_{\rm calculated} = C\left(\frac{1}{\tau_{\rm eff,\,FeB}} - \frac{1}{\tau_{\rm eff,\,Fe_i}}\right) \qquad (2)$$

with C being an injection dependent prefactor (positive) [18], [20] at $\Delta n = 1 \times 10^{15}$ cm^{-3}.

Finally, the error of the Fe estimation by the quasi-steady state photoconductance (QSSPC) method under the influence of an inhomogeneous Fe(x) profile was calculated by:

$$\text{Error \%} = \frac{[{\rm Fe}]_{\rm calculated} - [{\rm Fe}]_{\rm input\_avg}}{[{\rm Fe}]_{\rm input\_avg}} \times 100\% \qquad (3)$$

with $[{\rm Fe}]_{\rm input\_avg} = \frac{\int_0^W {\rm Fe}(x)dx}{W}$ being the average concentration of the input Fe(x) profile.

The degree of nonuniformity of the Fe depth profiles was defined using the normalized standard deviation of the Fe(x) distribution

$$\sigma = \frac{\sqrt{\int_0^W ({\rm Fe}^2\,(x) - [{\rm Fe}]_{\rm input\_avg}^2)dx}}{\sqrt{\int_0^W [{\rm Fe}]_{\rm input\_avg}^2\,dx}}. \qquad (4)$$

A perfectly uniform profile would give a σ of zero.

B. Input Fe(x) Profiles

The input inhomogeneous Fe depth profiles, Fe(x), are taken from simulations of a surface gettering process, which was based on numerically solving the diffusion equation with the boundary conditions defined by the segregation coefficient ($K_{\rm seg}$) of the surface gettering layers [11], [13], [23]. The segregation coefficient ($K_{\rm seg}$) is a key parameter that measures the effectiveness of the gettering sink. Specifically, $K_{\rm seg}$ is defined as the ratio of the Fe solubility in the gettering sink (e.g., phosphorus-doped layers) to the Fe solubility in the silicon wafer bulk [11]. A high $K_{\rm seg}$ indicates a high gettering capability of the gettering layer, as more Fe can be gettered to the layer. We assumed no diffusion barrier to reach the surface gettering sinks, and therefore the gettering rate is only limited by the Fe diffusivity in the Si wafer
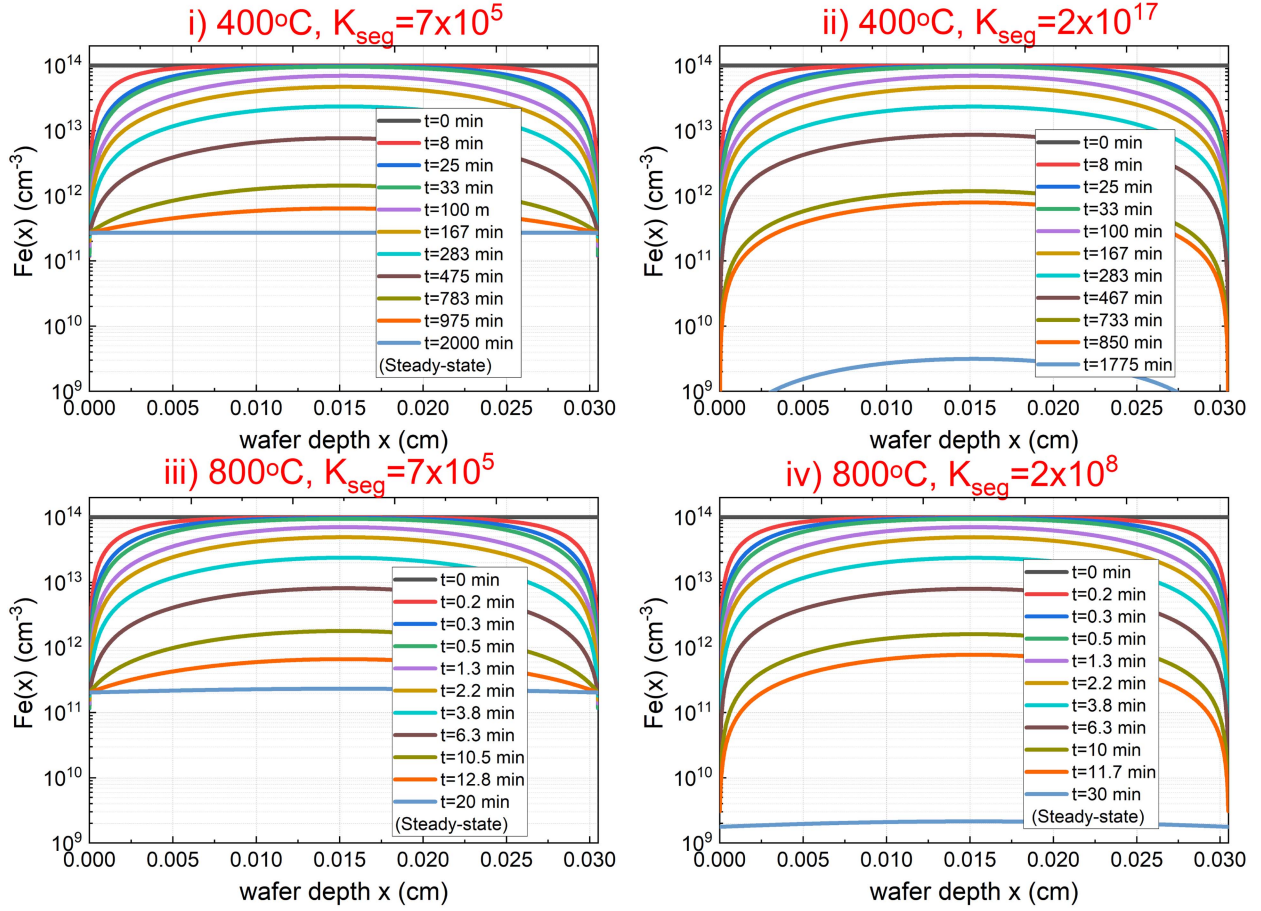
Fig. 1. Fe depth profiles (Fe(x)) at different time intervals during a gettering process for the four representative scenarios i, ii, iii, and iv.

bulk. The initial Fe depth profiles prior to gettering were assumed to be uniform, conditions often used in gettering studies. Based on our previous experimental gettering work, four representative scenarios were considered:

1) Relatively slow diffusion (at 400 °C), moderate surface gettering capability ($K_{seg} = 7 \times 10^5$).
2) Relatively slow diffusion (at 400 °C), practically infinite surface gettering capability ($K_{seg} = 2 \times 10^{17}$).
3) Fast diffusion (at 800 °C), moderate surface gettering capability ($K_{seg} = 7 \times 10^5$).
4) Fast diffusion (at 800 °C), strong surface gettering capability ($K_{seg} = 2 \times 10^8$).

The simulated Fe(x) profiles for the four scenarios are shown in Fig. 1. It can be observed from Fig. 1 that the initially homogeneous Fe depth profiles rapidly become inhomogeneous during a gettering process and eventually become homogeneous again at steady-state. Fig. 2(a) plots the corresponding average Fe concentration ($[Fe]_{input\_avg}$) as a function of the gettering time, and Fig. 2(b) plots the corresponding degree of nonuniformity [see (4)] as a function of $[Fe]_{input\_avg}$ for the four investigated scenarios.

As shown in Fig. 2(a), the early stages of the gettering process are the same for the samples with the same diffusion temperature (i.e., the same diffusivity) but different K_{seg} values. This is as expected because the diffusion of Fe in the Si wafer bulk is the rate-limiting factor in the modeled gettering process and the gettering kinetics only deviate significantly near the steady state conditions for the samples with a finite gettering capacity, that is, the gettering sink becomes saturated and the bulk [Fe] becomes uniform. Fig. 2(b) indicates that all four scenarios reach the same maximum level of Fe nonuniformity regardless of the Fe diffusivity (i.e., different temperatures) or the segregation coefficient of the gettering sinks, although they reach the maximum non-uniformity level at different gettering times and for different durations. That is, the maximum degree of Fe nonuniformity is accompanied by different average Fe concentrations, which may also affect the uniformity of the carrier depth profiles as demonstrated in Schubert et al. [10].

Further analyses of the profiles (not shown here) show that for the same $[Fe]_{input\_avg}$ and the same nonuniformity values, the Fe(x) profiles are identical in both the 400 °C and 800 °C cases.

Therefore, in this article, we will only further examine the simulation results related to scenario iv, which has more extreme Fe(x) profiles over a wider $[Fe]_{input\_avg}$ range. Simulations of Scenario ii were also performed and found to produce the same results (and are therefore not shown here). Scenario iv with different starting Fe concentrations were also considered, which would not change the shape of the Fe(x) profiles but only the magnitude.
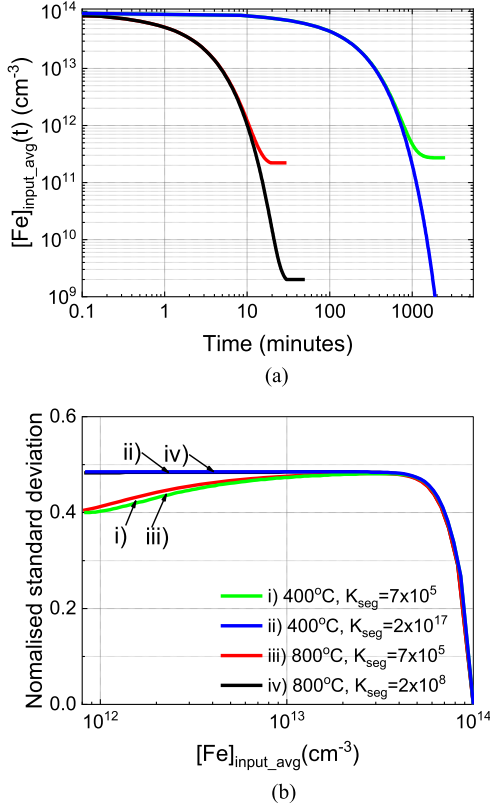
Fig. 2. (a) Average Fe concentration of the input Fe(x) profiles ([Fe]$_{\text{input\_avg}}$) as a function of gettering time ([Fe]$_{\text{input\_avg}}$(t)). (b) Degree of Fe profile nonuniformity, represented by the normalized standard deviation (σ), as a function of the average Fe concentration [Fe]$_{\text{input\_avg}}$, for the four representative scenarios i, ii, iii, and iv.

III. RESULTS AND DISCUSSION

A. Validation of the Model

To validate the model, the effective injection dependent lifetime curves simulated in this article using QsCell were compared with the lifetimes simulated from PC1D [24]. As can be seen from both the uniformly distributed Fe(x) scenario [see Fig. 3(a)] and the nonuniform step-like Fe(x) scenario [see Fig. 3(b)], the modeled injection-dependent lifetime curves show good agreement with the well-established PC1D. In principle, PC1D is sufficient to carry out the simulation for this article. However, in practice, we are unable to change the source code of PC1D to input a more realistic, smoothly varying Fe(x) profile that is not limited to a step function of five "steps."

B. Error Analyses for Uniform Fe Depth Profiles

To further validate the modeling procedure, we carried out an error analysis assuming homogeneous Fe(x) profiles, the same assumptions as in Schubert et al. [10]. Fig. 4 shows that the errors introduced to the lifetime-based Fe measurements (for both $W = 0.02$ cm and 0.03 cm wafers) are small, within 10% for a uniform Fe concentration of 10^{10} to 10^{14} cm^{-3}. This finding is similar to the previous results by Schubert et al. [10], who showed that the error in Fe estimation is small at a relatively strong illumination (required to reach an injection level of
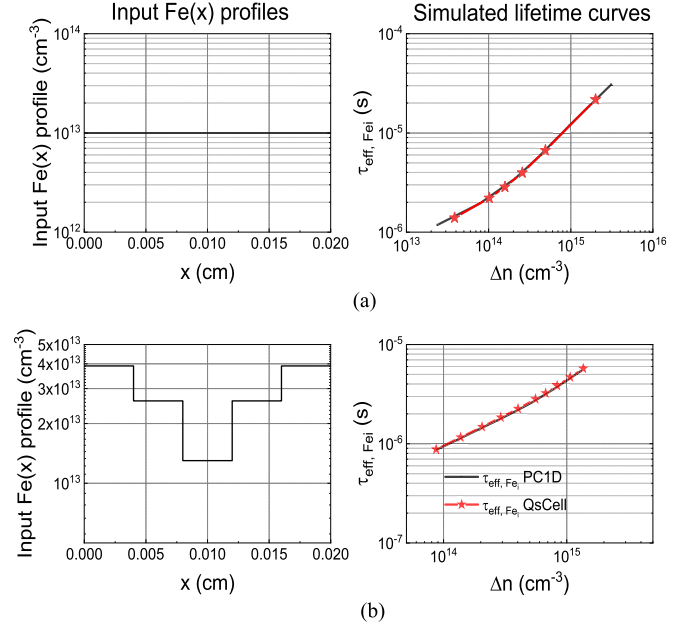

Fig. 3. Effective carrier lifetime curves simulated from PC1D and QsCell with (a) a uniformly distributed Fe(x) profile and (b) a nonuniform step-like Fe(x) depth profile. Both assumed a wafer thickness $W = 0.02$ cm.
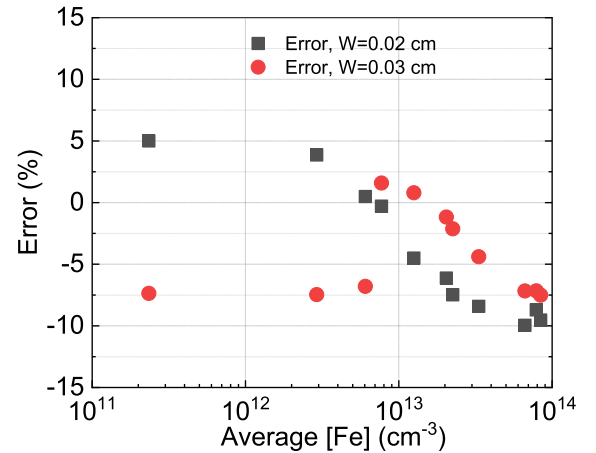

Fig. 4. Simulated errors for the uniformly distributed Fe(x) profiles at different Fe concentrations, assuming a 790 nm monochromatic light, at two wafer thicknesses of $W = 0.02$ cm and $W = 0.03$ cm, and $J_{0b} = J_{of} = 10^{-15} A cm^{-2}$.

$\Delta n = 1 \times 10^{15}$ cm^{-3} in low lifetime samples). For example, they showed that at [Fe] $= 1 \times 10^{13}$ cm^{-3} and illumination $\geq$ 10 suns, the error is in the range of 10% [10]. On the other hand, for the case of [Fe] $\leq 1 \times 10^{12}$ cm^{-3}, the condition of uniform carrier depth profiles is normally satisfied, and hence the errors in Fe estimation are small, which is consistent with our simulation in Fig. 4.

C. Error Analyses for Nonuniform Fe Depth Profiles

Fig. 5 compares the input ([Fe]$_{\text{input\_avg}}$) and calculated average Fe concentrations ([Fe]$_{\text{calculated}}$) from nonuniform Fe profiles during a gettering process (see Section II-B, scenario iv), assuming four different initial Fe concentrations. The difference between [Fe]$_{\text{input\_avg}}$ and [Fe]$_{\text{calculated}}$ is plotted as error [using
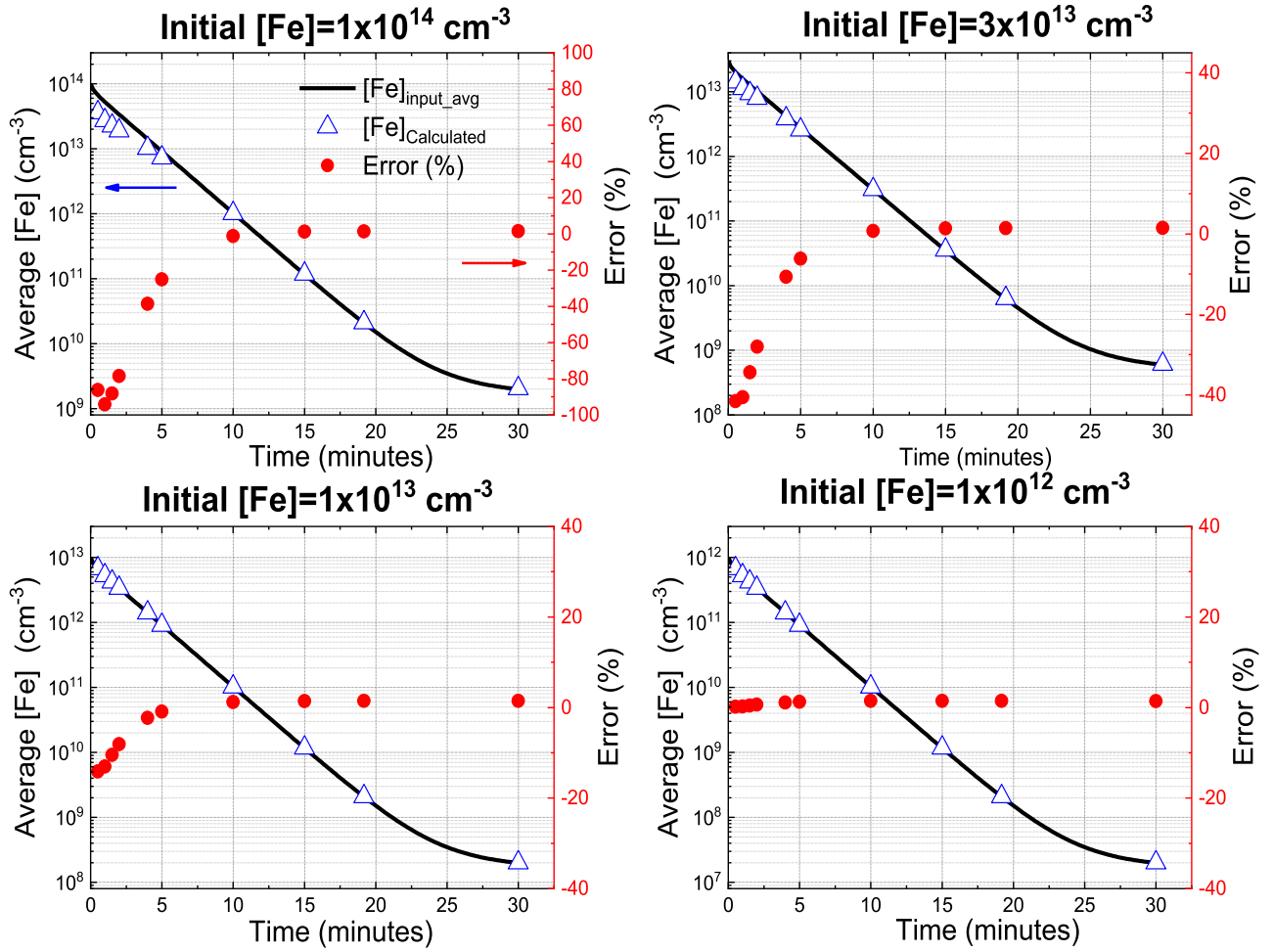
Fig. 5. Error analyses of different Fe(x) profiles during a gettering process. The assumed gettering process is 800 °C with strong gettering sinks of $K_{seg} = 2 \times 10^8$ on both wafer surfaces (i.e., Section II-B, scenario iv). Four different initial [Fe] (1×10^{14} cm^{-3}, 3×10^{13} cm^{-3}, 1×10^{13} cm^{-3}, and 1×10^{12} cm^{-3}) were assumed, with each plot showing a different initial [Fe]. All calculations were carried out assuming an Xenon flash spectrum as the light generation source and a well-passivated sample with $J_{0b} = J_{0f} = 10^{-15}$ Acm^{-2}. The solid lines illustrate the average values of the input Fe(x) profiles. The triangle symbols refer to the calculated Fe concentrations from QsCell. The red dots represent the error between [Fe]$_{input\_avg}$ and [Fe]$_{calculated}$ (3), and are plotted against the y-axis on the right.

(3)] in Fig. 5 as well. Comparing the errors from uniform Fe(x) (Fig. 4, wafer thickness W = 0.03 cm) and nonuniform Fe(x) profiles [see Fig. 5)], it can be seen that the errors are much more significant in the case of nonuniform Fe(x), especially at high Fe concentrations. At an average [Fe] close to 1×10^{14} cm^{-3}, inhomogeneous Fe(x) profiles can be underestimated by up to 100%, that is, half of the actual [Fe], as compared to only a 10% underestimation in the case of a homogenous Fe distribution. This clearly indicates that a nonhomogeneous Fe profile can introduce a significant additional error to the [Fe] measurement from QSSPC, particularly at high Fe concentrations above 1×10^{13} cm^{-3}. Care should be taken when working with such relatively high concentrations of Fe in silicon.

However, the errors are reduced with reducing Fe concentrations. As shown in Fig. 5, for an initial [Fe] of 3×10^{13}cm^{-3}, the maximum error is 40% underestimation of [Fe] (i.e., −40%), and this drops to −14% for an initial [Fe] of 1×10^{13}cm^{-3}. The errors are negligible for [Fe] below 1×10^{12} cm^{-3}. An initial [Fe] of 1×10^{13}cm^{-3} or below is common for defect and gettering studies, where small errors of less than ±14% are

expected. This result helps to validate the lifetime-based [Fe] measurements in our previous work (e.g., [13], [25]).

In general, the error of [Fe] measurement is dependent on both the Fe concentration in the Si wafer and the degree of non-uniformity of the Fe(x) profile (i.e., normalized standard deviation, σ). A higher Fe concentration and a more nonuniform Fe(x) profile lead to a higher error in [Fe] measurements from effective lifetime measurements.

To understand the reason behind such a significant underestimation in the [Fe] measurement in the case of a non-uniform Fe(x) profile, the corresponding generation and carrier depth profiles of an Fe(x) profile from the 3×10^{13}cm^{-3} gettering process is shown in Fig. 6, compared to the case of a uniform Fe(x) distribution of the same average Fe concentration (Fe$_{input\_avg}$).

As expected, the carrier depth profiles, $\Delta n(x)$, of the nonuniform Fe(x) scenario are more inhomogeneous compared to the $\Delta n(x)$ of the uniform Fe(x) case. The difference becomes larger in the FeB state. As the average Δn is kept constant in the Fe measurement, a lower generation rate, $G(x)$, is required to achieve the same average Δn in the FeB state, leading to a higher
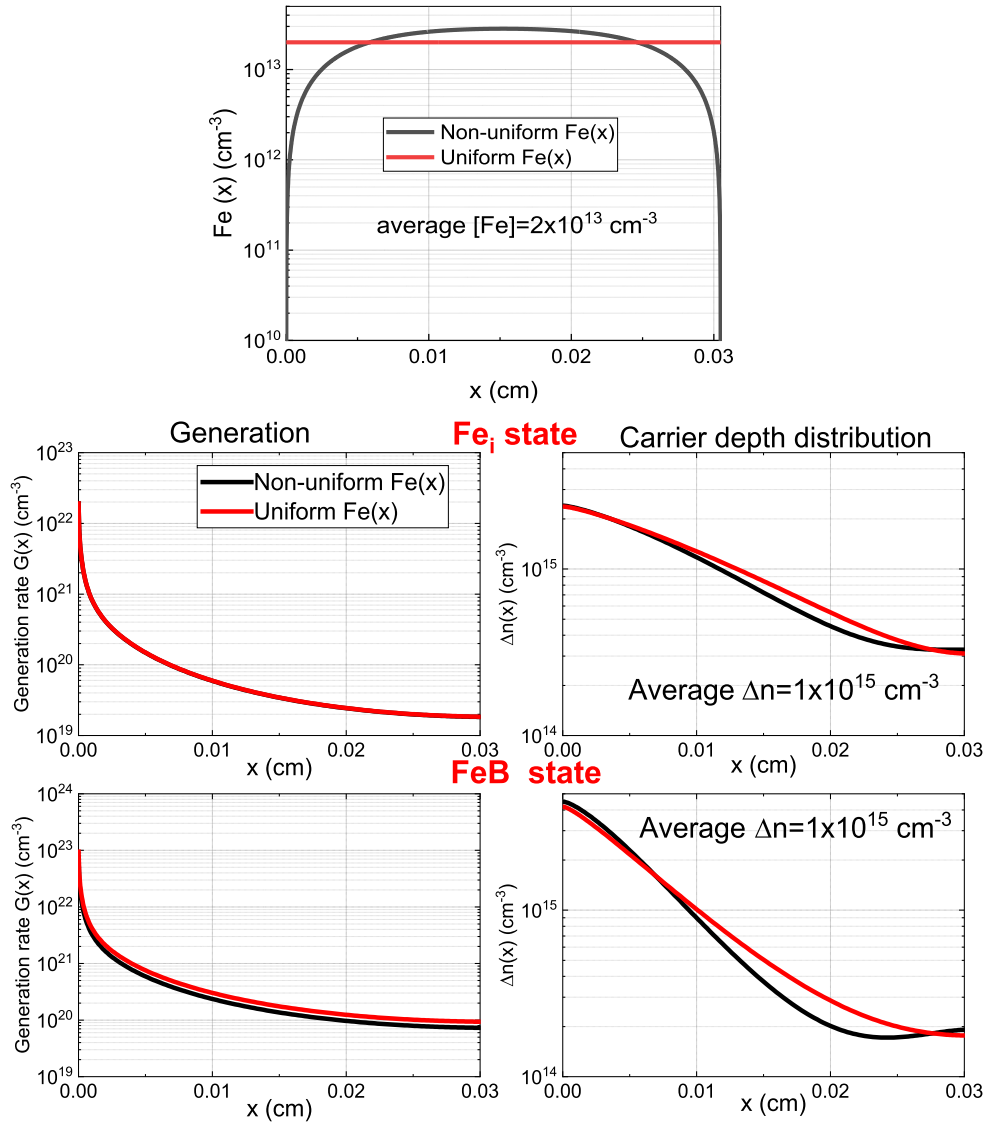
Fig. 6.   Input Fe(x) depth profiles in the Si bulk, and their corresponding generation rate $G(x)$ and carrier density profiles $\Delta n(x)$ from simulation. All calculations were carried out assuming an Xenon flash spectrum and a well-passivated sample with $J_{0b} = J_{0f} = 10^{-15}$ Acm^{-2}.
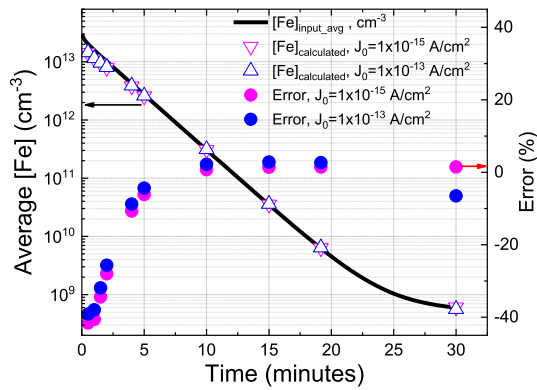

Fig. 7.   Effect of surface passivation, as represented by different J_0 values, on the error of [Fe] measurement. Here we assumed a sample with a starting [Fe] of 3×10^{13} cm^{-3}, undergoing an 800 °C gettering process (see Section II-B, scenario iv). All calculations were carried out assuming an Xenon flash spectrum. Errors are plotted against the y-axis on the right.
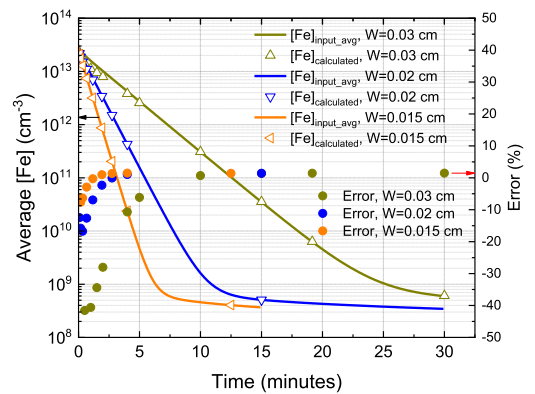
Fig. 8.   Error analysis of the effect of different wafer thickness (300, 200 and 150 μm), assuming a strong gettering process (see Section II-B, scenario iv) with an initial Fe concentration of 3×10^{13} cm^{-3}. All calculations were carried out assuming the Xenon flash spectrum and a well-passivated sample. Errors are plotted against the y-axis on the right.
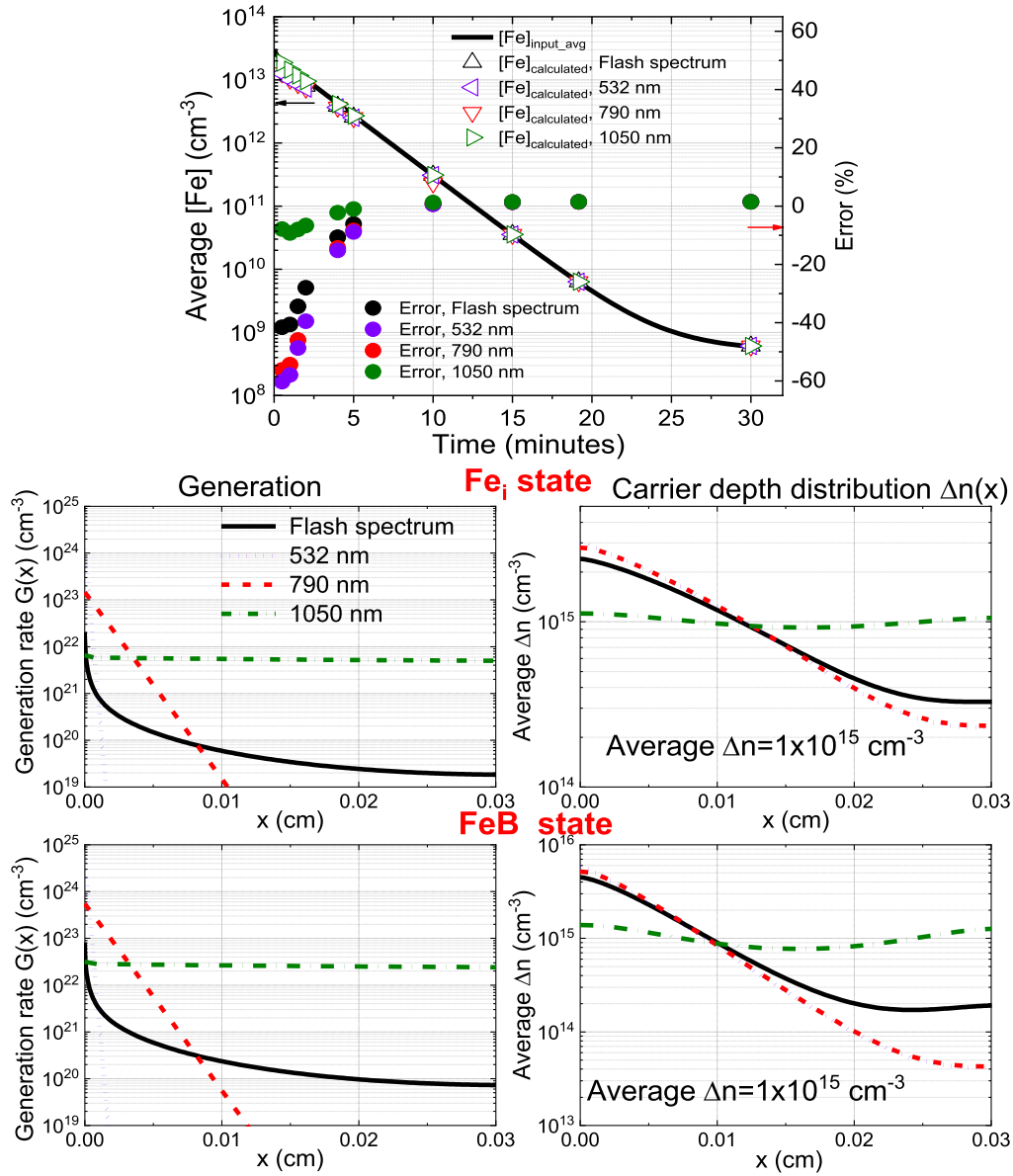
Fig. 9. Error analysis of the effect of four different light sources: one is the Xenon flash spectrum that is commonly used in Sinton lifetime testers, and the others are monochromatic illumination sources of 532, 790 and 1050 nm. Here we assumed a well-passivated ($J_{0b} = J_{0f} = 10^{-15}$ Acm^{-2}) sample with a starting bulk [Fe] of 3×10^{13} cm^{-3}, undergoing an 800 °C gettering process (see Section II-B, scenario iv).

$\tau_{\text{eff, FeB}}$ (1). On the other hand, in the Fe$_i$ state, the difference in the $\Delta n(x)$ profiles is smaller and so are the generation profiles $G(x)$. Therefore the calculated $\tau_{\text{eff, Fe}_i}$ values are similar in the Fe$_i$ state.

Consequently, the overestimated $\tau_{\text{eff, FeB}}$ in the case of a nonuniform Fe(x) profile leads to underestimated Fe concentration (2).

D. Effect of Other Factors

1) Effect of Surface Passivation: The effect of surface passivation was studied by changing the input J$_0$ value. Two representative cases of $J_{0b} = J_{0f} = 10^{-15}$ A/cm^2 for a well passivated sample and $J_{0b} = J_{0f} = 10^{-13}$ A/cm^2 for a poorly passivated sample were considered. In this case, the poorly passivated sample produced slightly lower error for the measured

[Fe] (see Fig. 7). This is as expected because a very high J_0 value is equivalent to a low surface lifetime, which is closer to the low bulk lifetime caused by the presence of Fe. As a result, the carrier depth profiles are smoother in the case of a poorly passivated sample (i.e., high J_0), leading to a slightly lower error in [Fe] measurement.

2) Effect of Wafer Thickness: Another factor that can affect the accuracy of the [Fe] measurement is the wafer thickness. In Fig. 8, the error analyses for three different wafer thicknesses of 300, 200 and 150 μm are shown with the assumed gettering process of in Section II-B, scenario iv and an initial [Fe] of 3×10^{13} cm^{-3}. As can be seen in Fig. 8, the error decreases with decreasing thickness: the maximum error is −40% for a 300 μm wafer, −17% for a 200 μm wafer, and −8% for a 150 μm wafer. The smaller error in a thinner wafer can also be explained by a more uniform carrier depth profile.

3) Effect of Illumination Source: The effect of different illumination sources on the [Fe] measurement error is simulated as well, as shown in Fig. 9. The different illumination sources include monochromatic 532, 790, and 1050 nm light sources and the commonly used Xenon flash spectrum [21] in a Sinton Instruments lifetime tester. As shown in Fig. 9, the 1050 nm monochromatic light source leads to the small errors, followed by the Xenon flash spectrum, and the 790 and 532 nm light sources demonstrate the largest errors. This can be explained by the different generation profiles inside the Si wafer bulk and the resulting carrier depth profiles. Fig. 9 shows that the 1050 nm light source results in the most uniform carrier depth profiles, followed by the Xenon flash spectrum, and the 790 and 532 nm light sources lead to the most inhomogeneous carrier profiles. An implication of this result is that using a longer wavelength illumination source can help to minimize the measurement error for samples with a low bulk lifetime and a non-uniform bulk defect distribution (with lower concentrations towards the front surface), through generating a more uniform carrier profile.

IV. CONCLUSION

Based on simulations using a modified version of QsCell [14], [15], [16], [17], this article quantifies the errors associated with Fe concentrations extracted from effective lifetime measurements, for silicon wafers with depth-wise inhomogeneous Fe distributions, and different Fe concentrations. The inhomogeneous Fe profiles are generated from simulations of surface gettering processes, which is the most representative scenario that causes significant Fe inhomogeneity in silicon wafers for solar cells. Our simulations illustrate that the error depends on both the average Fe concentration, which is consistent with the findings of Schubert et al. [10], and the nonuniformity of the Fe(x) profile in the Si wafer bulk. A significant error can be introduced due to a non-uniform Fe distribution: for example, assuming a 300-um thick silicon wafer, for an Fe gettering process with a starting Fe concentration of 1×10^{14} cm^{-3}, a large error of -100% (i.e., half of the actual average Fe concentration) can be observed in the initial stage of a gettering process (i.e., large inhomogeneity); this error is reduced to -40% for an initial Fe concentration of 3×10^{13} cm^{-3}; and this is further reduced to less than -15% if the initial Fe concentration is 1×10^{13} cm^{-3}, which is a value commonly used in our previous gettering studies. In the typical monocrystalline silicon wafers used for solar cell fabrication, the Fe concentration is mostly well below 10^{12} cm^{-3}, and the Fe concentration measurement error should be minimal. The error increases with increasing Fe concentration and increasing degree of non-uniformity of the Fe depth profiles, which are related to the non-uniformity of the carrier depth profiles in the Fe$_i$ and FeB states. Other factors such as surface passivation, illumination source and wafer thickness are also shown to affect the accuracy of Fe measurements.

REFERENCES

[1] A. A. Istratov, H. Hieslmair, and E. R. Weber, "Iron contamination in silicon technology," *Appl. Phys. A Mater. Sci. Process.*, vol. 70, no. 5, pp. 489–534, 2000.

[2] K. Graff, *Metal Impurities in Silicon-Device Fabrication*. Berlin, Germany: Springer, 2000.

[3] G. Zoth and W. Bergholz, "A fast, preparation-free method to detect iron in silicon," *J. Appl. Phys.*, vol. 67, no. 11, pp. 6764–6771, 1990.

[4] D. Macdonald, L. J. Geerligs, and A. Azzizi, "Iron detection in crystalline silicon by carrier lifetime measurements for arbitrary injection and doping," *J. Appl. Phys.*, vol. 95, no. 3, pp. 1021–1028, 2004.

[5] K. Wtinstel and P. Wagner, "Interstitial iron and iron-acceptor pairs in silicon," *Appl. Phys. A*, vol. 27, pp. 207–212, 1982.

[6] S. Pahlke, L. U. Fabry, L. Kotz, C. Mantler, and T. Ehmann, "Determination of ultra-trace contaminants on silicon wafer surfaces using total-reflection X-ray fluorescence TXRF 'state-of-the-art'," *Spectrochimica Acta Part B*, vol. 56, pp. 2261–2274, 2001.

[7] A. Corradi, M. Domenici, and A. Guaglio, "Surface contamination detection below the ppb range on silicon wafers," *J. Cryst. Growth*, vol. 89, pp. 39–42, 1988.

[8] L. Zhong and F. Shimura, "Dependence of lifetime on surface concentration of copper and iron in silicon wafers," *Appl. Phys. Lett.*, vol. 61, pp. 1078–1080, 1992.

[9] J. E. Birkholz, K. Bothe, D. Macdonald, and J. Schmidt, "Electronic properties of iron-boron pairs in crystalline silicon by temperature- and injection-level-dependent lifetime measurements," *J. Appl. Phys.*, vol. 97, no. 10, 2006, Art. no. 103708.

[10] M. C. Schubert, M. J. Kerler, and W. Warta, "Influence of heterogeneous profiles in carrier density measurements with respect to iron concentration measurements in silicon," *J. Appl. Phys.*, vol. 103, no. 11, 2008, Art. no. 073710.

[11] A. Liu, S. P. Phang, and D. Macdonald, "Gettering in silicon photovoltaics : A review," *Sol. Energy Mater. Sol. Cells*, vol. 234, 2022, Art. no. 111447.

[12] K. Mclean, C. Morrow, and D. Macdonald, "Activation energy for the hydrogenation of iron in p-type crystalline silicon wafers," in *Proc. IEEE 4th World Conf. Photovolt. Energy Conf.*, 2006, pp. 1122–1125.

[13] A. Liu et al., "Understanding the impurity gettering effect of polysilicon /oxide passivating contact structures through experiment and simulation," *Sol. Energy Mater. Sol. Cells*, vol. 230, 2021, Art. no. 111254.

[14] A. Cuevas and R. A. Sinton, "Detailed modelling of silicon solar cells," in *Proc. 23rd Eur. Photovol. Sol. Energy Conf. Exhib.*, 2008, pp. 315–319.

[15] A. Cuevas, "Modelling silicon characterisation," *Energy Procedia*, vol. 8, pp. 94–99, 2011.

[16] A. Cuevas and J. Tan, "Analytical and computer modelling of suns–Voc silicon solar cell characteristics," *Sol. Energy Mater. Sol. Cells*, vol. 93, pp. 958–960, 2009.

[17] A. Cuevas and R. A. Sinton, "Prediction of the open-circuit voltage of solar cells from the steady-state photoconductance," *Prog. Photovolt. Res. Appl.*, vol. 5, pp. 79–90, 1997.

[18] D. Macdonald, J. Tan, and T. Trupke, "Imaging interstitial iron concentrations in boron-doped crystalline silicon using photoluminescence," *J. Appl. Phys.*, vol. 103, no. 7, 2008, Art. no. 073710.

[19] A. A. Istratov, H. Hieslmair, and E. R. Weber, "Iron and its complexes in silicon," *Appl. Phys. A Mater. Sci. Process.*, vol. 69, no. 1, pp. 13–44, 1999.

[20] D. MacDonald, T. Roth, P. N. K. Deenapanray, T. Trupke, and R. A. Bardos, "Doping dependence of the carrier lifetime crossover point upon dissociation of iron-boron pairs in crystalline silicon," *Appl. Phys. Lett.*, vol. 89, no. 14, pp. 10–13, 2006.

[21] J. S. Swirhun, R. A. Sinton, M. K. Forsyth, and T. Mankad, "Contactless measurement of minority carrier lifetime in silicon ingots and bricks," *Prog. Photovolt. Res. Appl.*, vol. 19, pp. 313–319, 2011.

[22] R. A. Sinton and A. Cuevas, "Contactless determination of current-voltage characteristics and minority-carrier lifetimes in semiconductors from quasi-steady-state photoconductance data," *Appl. Phys. Lett.*, vol. 69, no. 17, pp. 2510–2512, 1996.

[23] H. Hieslmair, S. Balasubramanian, A. A. Istratov, and E. R. Weber, "Gettering simulator: Physical basis and algorithm," *Semicond. Sci. Technol.*, vol. 16, no. 7, pp. 567–574, 2001.

[24] D. A. Clugston and P. A. Basore, "PC1D version 5: 32-bit solar cell modeling on personal computers," in *Proc. IEEE Rec. Photovolt. Specialists Conf.*, 1997, pp. 207–210.

[25] T. T. Le et al., "Impurity gettering by silicon nitride films: Kinetics, mechanisms, and simulation," *Amer. Chem. Soc. Appl. Energy Mater.*, vol. 4, no. 10, pp. 10849–10856, 2021.